were broken but nuclei remained intact when analyzed under a microscope. A 30-μl sample of this homogenate was used for each assay. To the homogenate was added 1 μl (0.1 μg) of proteinase K or 1 μl of partially purified DCP-1. For inhibition of DCP-1, 0.1 mM Ac-DEVD-CHO was added with DCP-1. After 3 hours of incubation at 37°C, DNA was extracted and analyzed by agarose gel electrophoresis.

23. In situ hybridizations were performed as described (6).
24. Chromosome in situ analysis was performed essentially as described [M. Ashburner, Drosophila: *A Laboratory Manual* (Cold Spring Harbor Laboratory, Cold Spring Harbor, NY, 1989), protocol 27]. A DCP-1 biotinylated probe was hybridized to the wild type as well as the three deletion strains shown in Fig. 4. A collection of preexisting *P* element insertions mapping to the 59E-F region were crossed to these deletion strains for complementation analysis and were further analyzed by Southern (DNA) blot hybridization. Two *P* element strains, l(2)02132 and l(2)01862, showed alterations on a Southern blot when probed with the DCP-1 cDNA. The position and orientation of the two *P* elements in the DCP-1 gene were confirmed by PCR by using a 3′ *P* element primer and a primer within the DCP-1 coding region, and DNA sequencing of the PCR products. The Df(2R)G10-BR27 and Df(2R)bw^{DRa} stocks were received from B. Reed. *P* element strains were generated by the Berkeley *Drosophila* Genome Project and, together with Df(2R)bw^{5}, provided by the Bloomington Stock Center.
25. *P* element revertants were generated by standard genetic techniques. Viable and lethal revertants were recovered for both of the *P* element lines. Southern blot analysis was used to determine the presence of the *P* elements in the revertant lines.
26. Phenotypic analyses were performed on *dcp-1*^{1862}/*Df(2R)*bw^{DRa} transheterozygotes. These animals survive to various stages of larval development and display the melanotic tumor phenotype. The same phenotypes were also observed in *dcp-1*^{1862}/*dcp-1*^{2132} heterozygotes, and in larvae homozygous for a single transposon insertion. However, the *dcp-1*^{1862} chromosome appeared to contain additionally an unrelated background mutation that caused dorsal cuticle defects in embryos.
27. TUNEL labeling was carried out as described (9). This technique labels apoptotic nuclei by incorporating biotinylated nucleotides at the end of DNA double-strand breaks [Y. Gavrieli *et al.*, *J. Cell. Biol.* **119**, 493 (1992)]. In addition, antibody staining against the ENGRAILED protein was used to check for the presence of supernumerary cells in the CNS [L. Zhou *et al.*, *Curr. Biol.* **5**, 784 (1995)].
28. Z. Song and H. Steller, unpublished observations; A. Fraser and G. Evan, personal communication.
29. K. L. Watson *et al.*, *Dev. Genet.* **12**, 173 (1991); J. Sparrow, in *The Genetics and Biology of* Drosophila *2b*, M. Ashburner and T. R. Wright, Eds. (Academic Press, New York, 1978).
30. C. B. Thompson, *Science* **267**, 1456 (1995).
31. J. Campos-Ortega and V. Hartenstein, *The Embryonic Development of* Drosophila melanogaster (Springer-Verlag, New York, 1985).
32. We thank J. Yuan for providing the pactβgal vector and suggestions; D. Xue for a gift of CED-3 protein and advice; C. Hynds for assistance with figures; B. Reed, K. Matthews, and the Bloomington Stock Center for *Drosophila* stocks; the Berkeley *Drosophila* Genome Project for information on the *P* element strains; and K. Watson and C. Dearolf for useful advice. Supported by the American Cancer Society (K.M.). Z.S. is a postdoctoral associate and H.S. is an associate investigator of the Howard Hughes Medical Institute.

15 October 1996; accepted 3 December 1996

Requirement for the Transcription Factor LSIRF/IRF4 for Mature B and T Lymphocyte Function

Hans-Willi Mittrücker, Toshifumi Matsuyama, Alex Grossman, Thomas M. Kündig, Julia Potter, Arda Shahinian, Andrew Wakeham, Bruce Patterson, Pamela S. Ohashi, Tak W. Mak*

Lymphocyte-specific interferon regulatory factor (LSIRF) (now called IRF4) is a transcription factor expressed only in lymphocytes. Mice deficient in IRF4 showed normal distribution of B and T lymphocyes at 4 to 5 weeks of age but developed progressive generalized lymphadenopathy. IRF4-deficient mice exhibited a profound reduction in serum immunoglobulin concentrations and did not mount detectable antibody responses. T lymphocyte function was also impaired in vivo; these mice could not generate cytotoxic or antitumor responses. Thus, IRF4 is essential for the function and homeostasis of both mature B and mature T lymphocytes.

Lymphocyte-specific interferon regulatory factor (LSIRF) [now called IRF4 (*1*)] is a lymphocyte-restricted member of the interferon regulatory factor (IRF) family of transcription factors (*2*–*4*). This family is defined by a characteristic DNA binding domain and the ability to bind to the interferon-stimulated response element. Members of the IRF family are involved in diverse processes such as pathogen response, cytokine signaling, apoptosis, and control of cell proliferation (*5*).

We generated mice deficient in IRF4 by replacing exons 2 and 3 of the IRF4 gene with a neomycin resistance gene (*6*). Mouse strains derived from two independent embryonic stem cell lines exhibited an identical phenotype. Mutation of the IRF4 gene was confirmed by Southern (DNA) blot analysis of tail DNA (shown for one mouse strain in Fig. 1A). Hind III–digested DNA from $IRF4^{+/-}$ and $IRF4^{-/-}$ mice displayed the 3.3-kb band of the mutant locus; the wild-type band at 8.4 kb was absent in $IRF4^{-/-}$ mice. The absence of the IRF4 protein was confirmed by protein immunoblot analysis (Fig. 1B).

At 4 to 5 weeks of age, lymph nodes and spleens of $IRF4^{-/-}$ mice showed a relatively normal lymphocyte distribution and cellularity as compared with those of control littermates (Fig. 1C). At 10 to 15 weeks, spleens were enlarged 3 to 5 times and lymph nodes were enlarged 10 times over those of control littermates, because of an expansion of T (both $CD4^+$ and $CD8^+$) and B lymphocytes (Fig. 1C). The distribution of several different V_β-elements of the TCR was conserved, excluding the expansion of single T cell clones. Analysis of T cell surface molecules, including CD2, CD11a, CD18, CD25, CD28, CD45, CD54, FAS, and Thy-1, did not reveal any changes, although a slight increase in the number of $CD69^+$ T cells was observed. Thymi of $IRF4^{-/-}$ mice were of normal size and showed a normal distribution of thymic cell populations (Fig. 1C) (*7*).

Analysis of B lymphocytes from bone marrow revealed no differences in the expression of the B cell surface molecules CD43, immunoglobulin M (IgM), IgD, Igκ, B220, and I-A, indicating that early B cell development was grossly normal. The development of peritoneal $CD5^+$ B1 B cells was also normal (*7*). Splenic B cells showed normal surface expression of IgM and of κ and λ light chains (Fig. 2). However, on closer examination, spleens from $IRF4^{-/-}$ mice were found to display increased membrane IgM $(mIgM)^{high}$ $mIgD^{low}$, and decreased $mIgM^{low}$ $mIgD^{high}$, B cell populations. The frequency of $CD23^+$ $B220^+$ B cells was markedly reduced, and the $CD23^{high}$ $B220^+$ B cell subpopulation was absent (Fig. 2), indicating a block at a late stage of peripheral B cell maturation (*8*). Consistent with such a block was the absence of germinal centers in B cell follicles of spleens and lymph nodes, even after the injection of sheep red blood cells, a stimulus that induces a large number of germinal centers in control mice (*9*). Furthermore, plasma cells could not be detected in the spleen or lamina propria of $IRF4^{-/-}$ mice.

H.-W. Mittrücker, A. Grossman, T. M. Kündig, J. Potter, A. Shahinian, A. Wakeham, P. S. Ohashi, T. W. Mak, Departments of Immunology and Medical Biophysics, University of Toronto, and the Amgen Institute, 610 University Avenue, Toronto, Ontario, M5G 2C1, Canada.
T. Matsuyama, Department of Oncology, Faculty of Medicine, Nagasaki University, Nagaskai, Japan.
B. Patterson, Department of Oncologic Pathology, Ontario Cancer Institute, 610 University Avenue, Toronto, Ontario, M5G 2C1, Canada.
*To whom correspondence should be addressed.

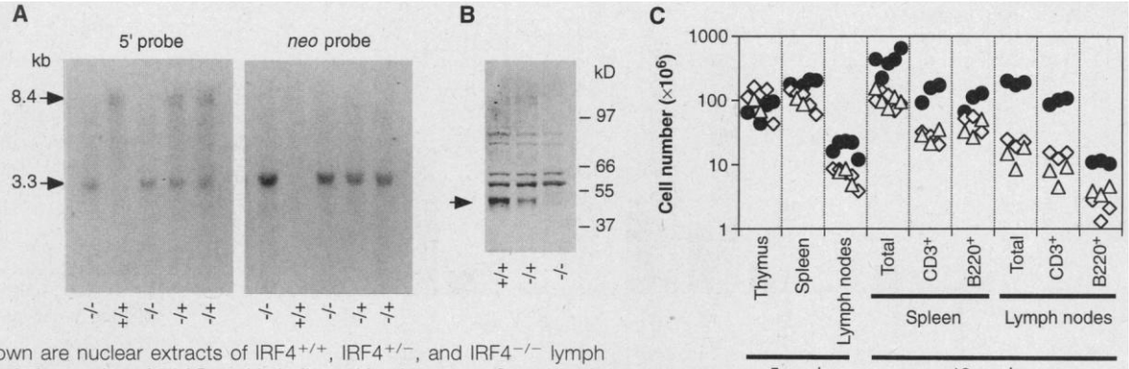

Fig. 1. Gene targeting of the murine IRF4 locus. (**A**) Southern blot analysis of mouse tail DNA. DNA was digested with Hind III and hybridized with the 5′ probe or with a *neo* probe. (**B**) Protein immunoblot analysis of concanavalin A (Con A)–activated lymph node cells with an antiserum specific for the COOH-terminus of IRF4 (*2*). Shown are nuclear extracts of IRF4$^{+/+}$, IRF4$^{+/-}$, and IRF4$^{-/-}$ lymph node cells. The IRF4 protein has a size of 51 kD and is indicated by the arrow. Cytoplasmic extracts were negative for IRF4 and are not shown. (**C**) Cellularity of spleen and lymph nodes in IRF4$^{-/-}$ mice. Cells from the thymus, spleen, and mesenteric lymph nodes were analyzed as described (*16*). IRF4$^{+/+}$, triangles; IRF4$^{+/-}$, diamonds; and IRF4$^{-/-}$, solid circles.

Serum concentrations in IRF4$^{-/-}$ mice of all Ig subclasses were reduced at least 99% (Fig. 3A). Although control mice immunized with dinitrophenyl keywhole limpet hemocyanin (DNP-KLH) showed strong DNP-specific Ig production (Fig. 3B), IRF4$^{-/-}$ mice produced no detectable hapten-specific antibodies (Abs). Antibody production was also absent when IRF4$^{-/-}$ mice were immunized with the T-independent antigen trinitrophenyl-lipopolysaccharide (TNP-LPS) (Fig. 3C).

To examine B cell activation, we stimulated purified B cells from control and IRF4$^{-/-}$ mice with Ab to IgM (anti-IgM), anti-CD40, or LPS (Fig. 4A). Whereas control B cells showed a proliferative response after anti-IgM or LPS stimulation, proliferation of IRF4$^{-/-}$ B cells was reduced after LPS stimulation and absent after IgM stimulation. The addition of interleukin-4 (IL-4) could not restore the defective proliferation of IRF4$^{-/-}$ B cells. In contrast, stimulation with anti-CD40 induced an equal proliferative response in both IRF4$^{+/+}$ and IRF4$^{-/-}$ B cells. Immunoglobulin secretion in response to stimulation with LPS or monoclonal antibody (mAb) to CD40 was severely impaired in IRF4$^{-/-}$ B cells (Fig. 4B).

IRF4 is induced in T cells after T cell receptor stimulation (*2*). To examine the in vitro response of IRF4$^{-/-}$ T cells, we incubated lymph node cells with mAb to CD3, concanavalin A, or the bacterial superantigen staphylococcal enterotoxin A (SEA) and measured cell proliferation (Fig. 5A). Proliferation of IRF4$^{-/-}$ T cells was reduced after incubation with all three stimuli and was not restored by the addition of IL-2. In mixed lymphocyte reaction (MLR) experiments, purified IRF4$^{-/-}$ T cells (H-2^b) showed reduced proliferation against BALB/c spleen cells (*H*-2^d) (Fig. 5B), which is consistent with a defect intrinsic to IRF4$^{-/-}$ T cells. Furthermore, IRF4$^{-/-}$ spleen and peritoneal cells were able to process and present antigens to wild-type T cells (*10*), excluding impaired antigen presentation of IRF4$^{-/-}$ cells. When IRF4$^{-/-}$

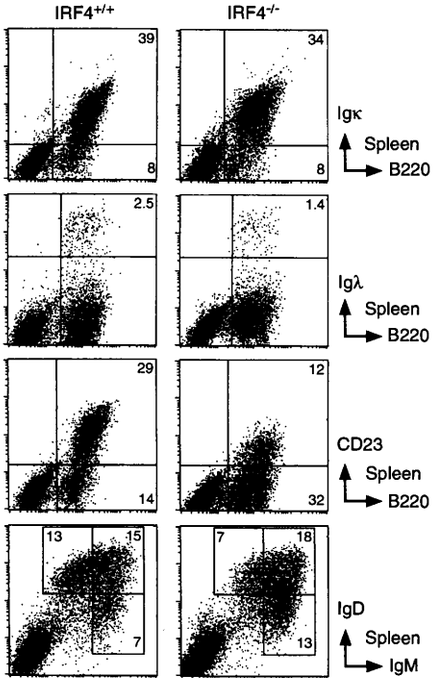

Fig. 2. Surface Ig and maturation markers in IRF4$^{-/-}$ B cells. Splenocytes were stained with fluorescein isothiocyanate—or phycoerythrin-conjugated mAbs to Igk, B220, CD23, IgD, and IgM or Abs to Igλ (anti-Igλ, Southern Biotech; all other mAbs, Pharmingen). Numbers indicate the percentage of cells in a quadrant or square. Staining and analysis were done as described (*16*).

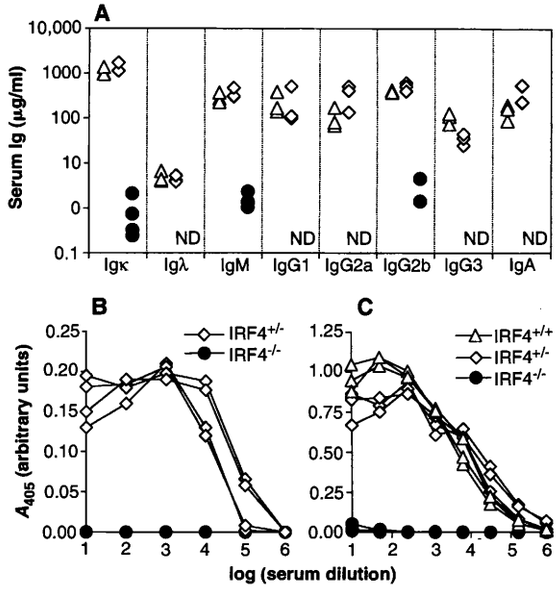

Fig. 3. Basal serum Ig concentrations, and responses to T-dependent and T-independent antigens in IRF4$^{-/-}$ mice. (**A**) Serum concentrations of different Ig subclasses were determined in 6- to 8-week-old mice by enzyme-linked immunosorbent assay (ELISA) (*16*). IRF4$^{+/+}$, triangles; IRF4$^{+/-}$, diamonds; IRF4$^{-/-}$, solid circles; ND, not detectable. (**B**) T-dependent antigens. IRF4$^{+/-}$ and IRF4$^{-/-}$ mice were injected subcutaneously with 100 μg of DNP-KLH in complete Freund's adjuvant and rechallenged on day 34 with 100 μg of DNP-KLH in incomplete Freund's adjuvant. Mice were bled, and hapten-specific IgG was determined by ELISA against DNP–bovine serum albumin (DNP-BSA). The results for day 44 are shown. A_{405}, absorbance at 405 nm. (**C**) T-independent antigens. Mice were injected ip with 100 μg of TNP-LPS. After 5 days, TNP-specific IgM was determined by ELISA against TNP-BSA (*17*).

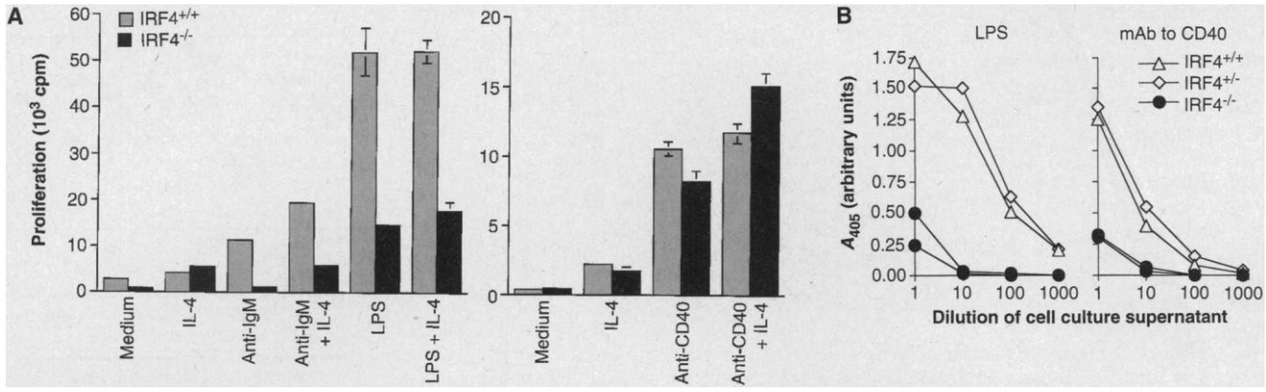

Fig. 4. (**A**) Proliferation of purified B cells after stimulation with IL-4, anti-IgM, LPS, or anti-CD40. Splenic B cells were purified by erythrocyte lysis and complement lysis of T cells as described (*18*). B cells (5×10^5 per well) were stimulated with LPS (10 μg/ml), goat anti-mouse IgM (20 μg/ml), anti-CD40 (5 μg/ml, clone 3/230), or mouse recombinant IL-4 (50 U/ml). Proliferation was measured at day 3 by [^{3}H]thymidine incorporation (*16*). Values are the mean of triplicate samples. (**B**) Antibody production after B cell stimulation with LPS and mAb to CD40 in vitro. Conditions were as described in (A). Total Ig was measured by ELISA after 3 days (*16*). Each experiment in (A) and (B) is representative of at least three independent experiments.

T cells were stimulated with mAb to CD3, the production of IL-2, IL-4, and interferon-γ (IFN-γ) was also found to be reduced (Fig. 5C).

To analyze the function of T cells in vivo, we infected IRF4$^{-/-}$ mice with lymphocytic choriomeningitis virus (LCMV). When injected into the footpads of normal mice, LCMV induces a strong cytotoxic T cell response, characterized by an immunopathologic swelling reaction which, in the early phase, is mediated by CD8$^+$ T cells (*11*). LCMV was injected into the footpads of mice, and after 8 days, spleen cells were analyzed for LCMV-specific cytotoxic activity (Fig. 5D). In contrast to cells from control mice, cells from IRF4$^{-/-}$ mice had no cytotoxic activity. In addition, whereas control mice showed the expected strong swelling of their footpads, swelling was absent in IRF4$^{-/-}$ mice.

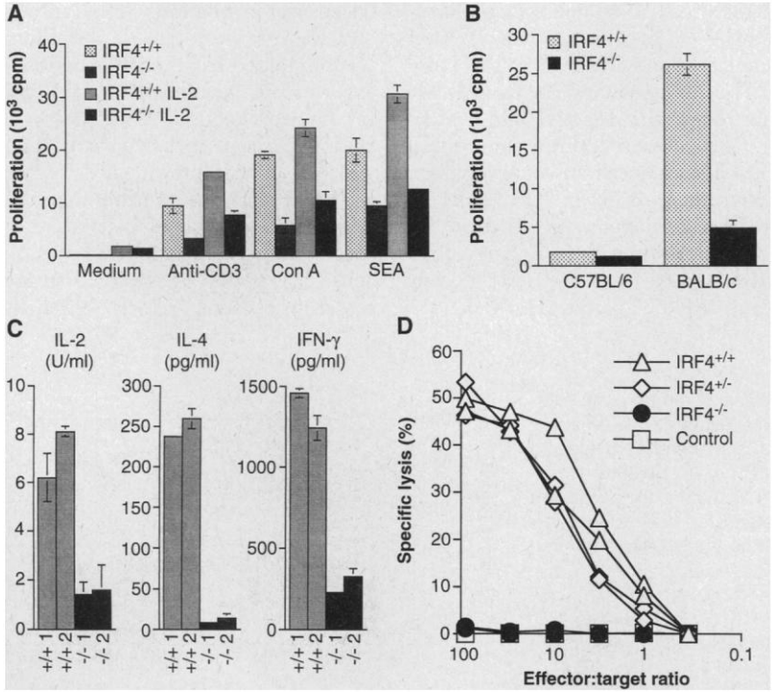

Fig. 5. In vitro and in vivo T cell responses of IRF4$^{-/-}$ mice. (**A**) Proliferation of lymph node T cells after stimulation with mAb to CD3ε, Con A, and SEA. (**B**) Mixed lymphocyte reaction. (**C**) Cytokine production after stimulation with mAb to CD3ε. (**D**) Cytotoxic response against LCMV (the control was an uninjected mouse). Proliferation after stimulation with Con A (2 μg/ml), anti-CD3ε (clone 145 2C11, 10 μg/ml), SEA (1 μg/ml), and IL-2 (50 U/ml) and MLR assays were performed as described (*16, 19*). For the MLR assays, T cells were purified with T cell enrichment columns (R&D Systems). For the induction of lymphokines, lymph node cells (4×10^6 per milliliter) were cultured for 48 hours in plates coated with anti-CD3ε (5 μg/ml) (*15*). IL-2 was determined with the CTLL-2 bioassay (*16*) and IL-4 and IFN-γ by ELISA (Genzyme). Values are the mean of triplicate samples. For determination of cytotoxic responses, mice were footpad-injected with 200 plaque-forming units of LCMV (Armstrong strain). Ex vivo cytotoxic activity of T cells was measured 8 days after infection in a ^{51}Cr-release assay with EL-4 target cells loaded with LCMV–glycoprotein peptide (amino acids 33 to 41) (*19*). Experiments in (A) through (D) are representative of at least three independent experiments, with at least three mice per group in (D).

The transplantation of T cells into an immunocompromized allogeneic host leads to a strong T cell–mediated graft-versus-host (GvH) reaction. BALB/c mice (*H-2^d*) with severe combined immunodeficiency disease (SCID) injected with spleen cells from allogeneic IRF4$^{+/+}$ and IRF4$^{+/-}$ mice (all H-2^b) developed a severe GvH reaction, accompanied by rough fur, overwhelming diarrhea, and massive weight loss (*12*). These mice died within 18 days of injection. Although SCID mice injected with allogeneic IRF4$^{-/-}$ cells displayed an initial weight loss, they recovered and survived for at least 40 days. Flow cytometric analysis revealed that after 4 weeks, the peripheral blood of these mice contained H-2K^{b+} donor-derived lymphocytes.

Finally, mice were injected with P815 mastocytoma cells, derived from DBA/2 mice (H-2^d). When injected into *H-2^b* mice, P815 cells are completely allogeneic and provoke a strong T cell response. All IRF4$^{+/+}$ and IRF4$^{+/-}$ mice were able to reject the P815 cells, and no tumor growth occurred for at least 3 months. In contrast, all IRF4$^{-/-}$ mice developed tumors with a time course identical to that seen in DBA/2 control mice (*13*).

It has been shown that IRF4 binds a motif in the Ig light chain gene enhancers

$E_{\kappa 3'}$, $E_{\lambda 2-4}$, and $E_{\lambda 3-1}$ and that IRF4 can enhance the transcription of genes under the control of this motif (3). For the κ-gene locus it has further been demonstrated that $E_{\kappa 3'}$ is crucial for κ–light chain secretion (*14*). Together, these facts could explain the defective Ig production in $IRF4^{-/-}$ mice. However, it is not likely that impaired light chain expression alone accounts for the severe B cell defect, and it is probable that IRF4 is involved in the expression of other genes that are important for late B cell differentiation.

In T cells, the deficiency of IRF4 leads to reduced proliferation and lymphokine production, and the reduced proliferation cannot be restored by exogenous IL-2. Analysis of early events after T cell activation, such as calcium influx or the expression of the activation molecules CD25 and CD69, revealed no difference between $IRF4^{-/-}$ and control T cells (*7*). Therefore, we conclude that IRF4 is not involved in the early events after T cell activation but is important for later processes, including both IL-2 production and IL-2 response, which is consistent with the strong up-regulation of IRF4 mRNA shortly after T cell activation (*2*).

Paradoxically, even though B and T cell responses are impaired in $IRF4^{-/-}$ mice, these animals develop severe lymphadenopathy. A possible explanation is that the incomplete lymphocyte activation in $IRF4^{-/-}$ mice affects the mechanisms controlling lymphocyte homeostasis, a phenomenon that has been described for IL-2– and IL-2Rα–deficient mice (*15*).

REFERENCES AND NOTES

1. Here we use the name IRF4, which was suggested and adopted for LSIRF by the nomenclature committee of the Genome Data Base for the gene locus in humans.
2. T. Matsuyama *et al.*, *Nucleic Acids Res.* **23**, 2127 (1995).
3. C. F. Eisenbeis, H. Singh, U. Storb, *Genes Dev.* **9**, 1377 (1995).
4. T. Yamagata *et al.*, *Mol. Cel. Biol.* **16**, 1283 (1996); A. Grossman *et al.*, *Genomics* **37**, 229 (1996).
5. M. Lamphier and T. Taniguchi, *Immunologist* **2**, 167 (1994); G. C. Sen and R. M. Ranshoff, *Adv. Virus Res.* **42**, 57 (1993); N. Tanaka *et al.*, *Nature* **382**, 816 (1996); P. S. Vaughan *et al.*, *ibid.* **377**, 362 (1995); N. Tanaka *et al.*, *Cell* **77**, 829 (1994); T. Tamura *et al.*, *Nature* **376**, 596 (1995); R. Kamijo *et al. Science* **263**, 1612 (1994).
6. To construct the targeting vector, an 8.4-kb Hind III fragment containing the promoter and exons 1 to 6 of the IRF4 gene was isolated from a 129J genomic library (*1*). The neomycin resistance cassette of pKJ1 (*neo*) [V. L. J. Tybulewicz *et al.*, *Cell* **65**, 1153 (1991)]; a Bam HI–Hind III fragment containing IRF4 exons 4, 5, and 6 (long arm); and a polymerase chain reaction (PCR) fragment of intron 1 (short arm) were sequentially cloned into pBluescript SK. The targeting vector was linearized, and E14 embryonic stem (ES) cells were transfected and selected with G418. Targeted ES cell colonies were screened by PCR with primers specific for the 3′ region of *neo* and for a genomic sequence 5′ of the targeting construct. Positive ES cell lines were verified by Southern hybridization after Hind III digestion, with the use of probes specific for a sequence 5′ of the short arm (5′ probe) or for *neo*. Out of 1500 G418-resistant colonies, we could isolate 8 with the correct mutation and with a single *neo* integration. Positive ES cells were injected into CD1 blastocysts, and chimeric offspring were mated with C57BL/6 female mice. Mice were screened by Southern blot analysis or by PCR of tail DNA with the primers 5′-GCA ATG GGA AAC TCC GAC AGT-3′ and 5′-CAG CGT CCT CCT CAC GAT TGT-3′, specific for exon 2; and primers 5′-CCG GTG CCC TGA ATG AAC TGC-3′ and 5′-CAA TAT CAC GGG TAG CCA ACG-3′, specific for *neo*.
7. H.-W. Mittrücker, unpublished observations.
8. R. Carsetti, G. Köhler, M. Lamers, *J. Exp. Med.* **181**, 2129 (1995).
9. To induce the formation of germinal centers, mice were injected intraperitoneally (ip) with sheep red blood cells (1×10^9) in 100 ml of phosphate-buffered saline (PBS) and killed 10 days later. Tissues were fixed in formalin and embedded in paraffin. Sections were stained with hematoxylin-eosin.
10. In MLR experiments, $IRF4^{+/+}$ and $IRF4^{-/-}$ spleen cells induced equal proliferation in allogeneic T cells. Furthermore, $IRF4^{-/-}$ peritoneal and spleen cells demonstrated no impairment in the processing and presentation of ovalbumin to ovalbumin-specific T cells or of LCMV peptides, after LCMV infection, to LCMV-specific T cells.
11. T. P. Leist, S. P. Cobbold, H. Waldmann, M. Aguet, R. M. Zinkernagel, *J. Immunol.* **138**, 2278 (1987); D. Moskophidis and F. Lehmann-Grube, *Proc. Natl. Acad. Sci. U.S.A.* **86**, 3291 (1989).
12. BALB/c-SCID mice (bred in-house at the Ontario Cancer Institute) were sublethally irradiated (400 rad), immediately injected intravenously with 5×10^7 spleen cells in 500 ml of PBS, and weighed every second day. In two independent experiments, 2, 5, and 10 BALB/c-SCID mice were injected with $IRF4^{+/+}$, $IRF4^{+/-}$, or $IRF4^{-/-}$ spleen cells, respectively. Mice were tail-bled, and cells were stained with mAb to H-$2K^b$ and analyzed by flow cytometry.
13. P815 cells (6×10^3 cells per mouse) were injected ip into $IRF4^{+/+}$, $IRF4^{+/-}$, and $IRF4^{-/-}$ mice (all H-2^b) and DBA/2 control mice (H-2^d). Mice (at least five mice per group) were monitored daily and killed when ascites development was visible (17 to 20 days after injection).
14. K. B. Meyer, M. J. Sharpe, M. A. Surani, M. S. Neuberger, *Nucleic Acids Res.* **18**, 5609 (1990); A. G. Betz *et al.*, *Cell* **77**, 239 (1994).
15. D. M. Willerford *et al.*, *Immunity* **3**, 521 (1995); B. Kneitz, T. Herrmann, S. Yonehara, A. Schimpl, *Eur. J. Immunol.* **25**, 2572 (1996).
16. A. Shahinian *et al.*, *Science* **261**, 609 (1993); H.-W. Mittrücker *et al.*, *J. Exp. Med.* **183**, 2481 (1996).
17. P. Mombaerts *et al.*, *Int. Immunol.* **6**, 1061 (1994).
18. T. Benatar *et al.*, *J. Exp. Med.* **183**, 329 (1996).
19. R. Schmits *et al.*, *ibid.*, p. 1415.
20. Healthy 5- to 7-week-old mice were used for all experiments. Mice were maintained according to the guidelines of the Canadian Council of Animal Care. H.-W.M. is a recipient of a grant from the Deutsche Forschungsgemeinschaft. The authors thank M. Bachmann, G. Boehmelt, G. Duncan, D. Ferrick, C. Furlonger, D. Kägi, F. Kiefer, L. Marengere, C. Paige, J. Penninger, M. Saunders, R. Schmits, D. Siderovski, D. Speiser, S. Yoshinaga, and P. Waterhouse for providing reagents and for helpful comments.

4 October 1996; accepted 2 December 1996

Still life, a Protein in Synaptic Terminals of *Drosophila* Homologous to GDP-GTP Exchangers

Masaki Sone, Mikio Hoshino,* Emiko Suzuki, Shinya Kuroda, Kozo Kaibuchi, Hideki Nakagoshi, Kaoru Saigo, Yo-ichi Nabeshima, Chihiro Hama†

The morphology of axon terminals changes with differentiation into mature synapses. A molecule that might regulate this process was identified by a screen of *Drosophila* mutants for abnormal motor activities. The *still life* (*sif*) gene encodes a protein homologous to guanine nucleotide exchange factors, which convert Rho-like guanosine triphosphatases (GTPases) from a guanosine diphosphate–bound inactive state to a guanosine triphosphate–bound active state. The SIF proteins are found adjacent to the plasma membrane of synaptic terminals. Expression of a truncated SIF protein resulted in defects in neuronal morphology and induced membrane ruffling with altered actin localization in human KB cells. Thus, SIF proteins may regulate synaptic differentiation through the organization of the actin cytoskeleton by activating Rho-like GTPases.

The morphology of synaptic terminals changes during synaptogenesis and in response to environmental cues or neural activity (*1*). Rho-like GTPases, which include Rac1, Cdc42, and Rho, regulate cell motility, morphology, and adhesion through interaction with the actin cytoskeleton (*2*), and they are also implicated in the extension or elaboration of axons and dendrites in the nervous system (*3*, *4*). Here we describe the Still life (SIF) proteins of *Drosophila* that participate in the signaling cascade of the Rho-like GTPases in the synaptic terminals.

To identify factors involved in the formation of neural circuits, we created *Drosophila* mutants by the insertion of an enhancer trap transposon and then screened them for reduced locomotor behavior, an approach used to identify factors that function during synapse formation (*5*, *6*). We isolated a mutant, $sif^{98.1}$, that carries a single *P* element insertion at the cytological location 64E. Flies homozygous for this insertion demonstrated reduced locomotion (Fig. 1A) and were male sterile.

We isolated genomic DNA surrounding